



TITLE:

^{13}C NMR Analysis of the α -Methyl Group Rotation of Solid Poly(methyl methacrylate)s with Different Tacticities (Commemoration Issue Dedicated to Professor Hiroshi Ibagaki, Professor Michio Kurata, Professor Ryozo Kitamura, On the Occasion of The ...

AUTHOR(S):

Horii, Fumitaka; Chen, Yiyi; Nakagawa, Masaru; Gabry, Barbara; Kitamaru, Ryozo

CITATION:

Horii, Fumitaka ...[et al]. ^{13}C NMR Analysis of the α -Methyl Group Rotation of Solid Poly(methyl methacrylate)s with Different Tacticities (Commemoration Issue Dedicated to Professor Hiroshi Ibagaki, Professor Michio Kurata, Professor Ryozo Kita ...

ISSUE DATE:

1989-02-15

URL:

<http://hdl.handle.net/2433/77230>

RIGHT:

^{13}C NMR Analysis of the α -Methyl Group Rotation of Solid Poly(methyl methacrylate)s with Different Tacticities

Fumitaka HORII*, Yiyi CHEN**, Masaru NAKAGAWA*,
Barbara GABRYŠ***, and Ryozyo KITAMARU*

Received November 20, 1988

^{13}C spin-lattice relaxation times $T_{1\text{C}}$ of the α -methyl groups of amorphous poly(methyl methacrylate) samples with different tacticities have been measured over a wide range of temperatures by cross-polarization/dipolar decoupling ^{13}C NMR spectroscopy. The $T_{1\text{C}}$ minimum has been clearly observed for each sample, but the temperature dependences of the $T_{1\text{C}}$ values, especially the temperature at which $T_{1\text{C}}$ reaches the minimum, greatly depend on the tacticities of the samples. Such characteristic temperature dependences of the $T_{1\text{C}}$'s have been analyzed in terms of the multiple-correlation-time models where the three-fold rotation of the α -methyl group and the rapid fluctuation of the rotation axis are assumed to describe the motion of the C-H internuclear vector.

KEY WORDS: High-Resolution ^{13}C NMR/ α -Methyl Group Rotation/ Multiple-Correlation-Time Model/ Poly(methyl methacrylate)/ Tacticity/

INTRODUCTION

One decade ago Schaefer and Stejskal¹⁾ observed the first high-resolution solid-state ^{13}C NMR spectra of solid polymers. They combined three sophisticated techniques of ^{13}C - ^1H dipolar decoupling (DD), magic-angle sample spinning (MAS), and the ^1H - ^{13}C cross-polarization (CP), and therefore the operation of the solid-state NMR is considerably more complicated compared to that used to obtain the conventional NMR spectra in liquids. However, since this method, frequently termed the CP/MAS ^{13}C NMR spectroscopy, is very sensitive to the local molecular conformation and dynamics of polymers, it has become one of standard methods to characterize the structure and molecular motions of solid polymers.

We have investigated the phase structure and molecular mobility of crystalline solid polymers such as polyethylene,²⁻⁴⁾ polypropylene,⁵⁾ poly(vinyl alcohol),^{6, 7)} polyethers,⁸⁾ cellulose,⁹⁻¹¹⁾ and amylose¹²⁾ by CP/MAS ^{13}C NMR spectroscopy with particular emphasis laid on the separate characterization of the contributions from the crystalline and noncrystalline regions. For example, we have found for different polyethylene samples that the crystalline-amorphous interphase, which is defined as a transition region between the crystalline and amorphous regions, can be detected from the differences in ^{13}C spin-spin relaxation times T_2 as well as ^{13}C chemical shifts.²⁻⁴⁾ The exact separation of the contributions of the crystalline and noncrystalline compo-

* 堀井文敬, 中川 将, 北丸竜三: Laboratory of Fundamental Material Properties, Institute for Chemical Research, Kyoto University, Uji, Kyoto 611, Japan.

** 陳 宜宜: Changchun Institute of Applied Chemistry, Academia Sinica, Changchun, PRC.

*** Department of Physics, Brunel University of West London, Uxbridge, Middlesex UB8 3PH, UK.

nents to the NMR signal has also provided new information about the crystal structure of native cellulose. We have pointed out that the CP/MAS ^{13}C NMR spectra of the crystalline components of native cellulose can be approximately classified into two types, cotton-ramie and bacterial-valonia types.⁹⁻¹¹⁾ This analysis is consistent with the existence of two allomorphs for the crystal structure (cellulose I) of native cellulose, in good accord with the previous proposal of VanderHart and Atalla.^{12,13)}

The detailed analysis of the molecular motions of polymers have been performed mainly for the rubbery components forming part of the isothermally crystallized polyethylene^{14,15)} and polyesters¹⁶⁾ by the conventional ^{13}C NMR spectroscopy. The reason for the choice of this technique is that the ^{13}C spin relaxation parameters, such as spin-lattice relaxation time T_1 , T_2 , and nuclear Overhauser enhancement NOE , are very sensitive to the backbone motion in the rubbery state where the correlation time is of the order 10^{-12} – 10^{-5} s. We have prepared a model where a random fluctuation of the C-H internuclear vector is caused by several superposed motions with different correlation times. Such a multiple-correlation-time model gives a good agreement with the experimental relaxation when the main chain motion is described in terms of 3–4 types of motion.^{14,15)}

In this paper a multiple-correlation-time model has been applied to the analysis of the molecular motion of the α -methyl group in a number of poly(methyl methacrylate) (PMMA) samples with different tacticities in the glassy state. Since the characterization of methyl group rotation is a fundamental problem in molecular dynamics, a large body of data has already been collected using dielectric and dynamic mechanical relaxation,^{17,18)} pulsed and broad-line ^1H NMR,^{19,20)} ^{13}C NMR in solution^{21,22)} and in solids,²³⁻²⁵⁾ and inelastic and quasielastic neutron scattering.²⁶⁻²⁸⁾ However, the mechanism of rotation of the α -methyl group has not yet been understood completely. Our first report of the detection of the T_{1C} minimum for poly(methyl methacrylate)s has been published elsewhere.²⁹⁾

MULTIPLE-CORRELATION-TIME MODEL

^{13}C spin-lattice relaxation time T_{1C} for the ^{13}C - ^1H two spin system may be expressed as follows:

$$1/T_{1C} = [\gamma_C^2 \gamma_H^2 \hbar^2 / 16r^6] [J_0(\omega_H - \omega_C) + 18J_1(\omega_C) + 9J_2(\omega_H + \omega_C)] \quad (1)$$

assuming the magnetic dipole-dipole interaction between the two spins as a main cause of the relaxation. Here, γ_C and γ_H are the nuclear gyromagnetic ratios of the ^{13}C and ^1H nuclei, respectively, \hbar is the reduced Planck constant ($=h/2\pi$), r is the distance between the nuclei, and ω_C and ω_H are the ^{13}C and ^1H resonance frequencies. In this equation $J_q(\omega)$ are the spectral density functions, which are defined as the Fourier intensities of the correlation functions of the orientation functions F_q at frequency ω :

$$J_q(\omega) = \int_{-\infty}^{\infty} \langle F_q^*(t+\tau) F_q(t) \rangle \exp(-i\omega\tau) d\tau \quad (2)$$

with $q=0, 1$, and 2 .

The orientation functions F_q are given by :

$$\begin{aligned} F_0(t) &= 1 - 3n^2 \\ F_1(t) &= (1 + im)n \\ F_2(t) &= (1 + im)^2 \end{aligned} \quad (3)$$

Here l , m , and n are the direction cosines of the C-H internuclear vector with respect to the x , y , and z axes in the laboratory frame, respectively, the z axis being parallel to the direction of the static magnetic field. Since the C-H internuclear vector fluctuates due to the thermal motion of the system, $F_q(t)$ are time dependent via the temporal fluctuations of l , m , and n .

Many models describing thermal fluctuation of the direction cosines have already been proposed and the equations governing the spectral densities have been derived using these models. In the multiple-correlation-time models the thermal motion of the C-H internuclear vector is described in terms of the superposition of several independent random motions. Let S_1, S_2, \dots, S_{p-1} be the rectangular coordinates which are set in the respective moving units. Then, denote by S_1 the coordinate system to describe the most inner motion of the C-H internuclear vector and by S_p the laboratory frame. The direction cosines l , m , and n in the laboratory frame are then related to the direction cosines l_1 , m_1 , and n_1 of the C-H vector in coordinate S_1 by the following relationship :

$$\begin{pmatrix} l \\ m \\ n \end{pmatrix} = T_p \cdots T_3 T_2 \begin{pmatrix} l_1 \\ m_1 \\ n_1 \end{pmatrix} \quad (4)$$

where T_i are the matrices of the orthogonal transformation from frame S_{j-1} to frame S_j :

$$T_j = \begin{pmatrix} \cos \phi_j \cos \theta_j \cos \psi_j - \sin \phi_j \sin \psi_j \\ \sin \phi_j \cos \theta_j \cos \psi_j + \cos \phi_j \sin \psi_j \\ -\sin \theta_j \cos \psi_j \\ -\cos \phi_j \cos \theta_j \sin \psi_j - \sin \phi_j \cos \psi_j & \cos \phi_j \sin \theta_j \\ -\sin \phi_j \cos \theta_j \sin \psi_j + \cos \phi_j \cos \psi_j & \sin \phi_j \sin \theta_j \\ \sin \theta_j \sin \psi_j & \cos \theta_j \end{pmatrix} \quad (5)$$

Here, ϕ_j , θ_j , and ψ_j are the Euler angles which describe coordinate S_{j-1} in coordinate S_j . Therefore the thermal fluctuation of the C-H internuclear vector can be expressed in terms of the time fluctuations of the Euler angles in each frame in the multiple-correlation-time models.

We have already derived the exact equations for the spectral densities for the case $p=3$ ³⁰⁾ first proposed by Howarth.³¹⁾ As shown in Figure 1, in this model the C-H internuclear vector undergoes the diffusional rotation about the z_1 axis in frame S_1 and the z_1 axis librates within a cone whose axis is parallel to the z_2 axis in frame S_2 . Furthermore, the z_2 axis undergoes the isotropic random reorientation in the laboratory frame. This model turned out to be very useful for analyzing the characteristic temperature dependences of ^{13}C T_1 , T_2 , and NOE for noncrystalline chains included in

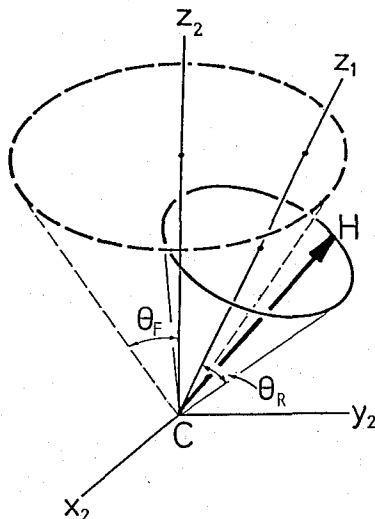


Fig. 1. A schematic diagram of the multiple-correlation-time model corresponding to the case of $p=3$.

polyethylene^{14,15)} and polyesters¹⁶⁾ isothermally crystallized from the melt or from a dilute solution.

The diffusional rotation about the z_1 axis, which was described above, is not a plausible model for the α -CH₃ rotation in PMMA. Therefore, we assume that the three-fold jump rotation of the C-H internuclear vector occurs about the z_1 axis in frame S_1 . The rapid fluctuation of the rotation axis (the z_1 axis) occurring in frame S_2 may be described by the librational motion used in the previous model,³⁰⁾ if the correlation time and the amplitude of the motion are appropriately adjusted to the values in the glassy state.

In the previous paper³⁰⁾ the spectral densities were derived for a special case but more general derivation is presented here. For models where three different superposed motions are assumed, Eq. (4) reduces to

$$\begin{pmatrix} l \\ m \\ n \end{pmatrix} = T_3 T_2 \begin{pmatrix} l_1 \\ m_1 \\ n_1 \end{pmatrix} \quad (6)$$

with

$$\begin{aligned} l_1 &= \cos \phi_1 \sin \theta_1 \\ m_1 &= \sin \phi_1 \sin \theta_1 \\ n_1 &= \cos \theta_1. \end{aligned} \quad (7)$$

If we assume random motions about the z_i axis in frames S_i , angles ϕ_i are set to zero in Eq. (5). Then, the orientation functions F_q given by Eq. (3) can be expressed in terms of the sum of the products of three functions f , g , and h , which are the functions of θ_1 and ϕ_1 , θ_2 and ϕ_2 , and θ_3 and ϕ_3 , respectively, as follows

$$F_q(t) = \sum_{j=1}^5 \sum_{k=1}^5 f^{(q)}_{jk}(t) g^{(q)}_{jk}(t) h^{(q)}_{jk}(t) \quad (8)$$

The explicit forms of functions $f^{(q)}_{jk}(t)$, $g^{(q)}_{jk}(t)$, and $h^{(q)}_{jk}(t)$ were given for each q in Table I of Ref. 30. Although those functions were derived for a particular case at that time, they are applicable to somewhat more general cases being considered here. Thus, the correlation functions of $F_q(t)$ are expressed by

$$\begin{aligned} & \langle F_q^*(t+\tau) F_q(t) \rangle \\ &= \langle [\sum_{j,k} f^{(q)}_{jk}{}^*(t+\tau) g^{(q)}_{jk}{}^*(t+\tau) h^{(q)}_{jk}{}^*(t+\tau)] \\ & \quad \times [\sum_{l,m} f^{(q)}_{lm}(t) g^{(q)}_{lm}(t) h^{(q)}_{lm}(t)] \rangle \\ &= \sum_{j,k} \sum_{l,m} \langle f^{(q)}_{jk}{}^*(t+\tau) f^{(q)}_{lm}(t) \rangle \langle g^{(q)}_{jk}{}^*(t+\tau) g^{(q)}_{lm}(t) \rangle \\ & \quad \times \langle h^{(q)}_{jk}{}^*(t+\tau) h^{(q)}_{lm}(t) \rangle. \end{aligned} \quad (9)$$

Here, the last equation in Eq. (9) is obtained by assuming the motions to be independent of each other. Moreover, as already mentioned, each motion is a random motion about the z_i axis, leading to the equal probabilities for ϕ_1 , ϕ_2 , and ϕ_3 in the ranges of $0 \leq \phi_1 \leq 2\pi$, $0 \leq \phi_2 \leq 2\pi$, and $0 \leq \phi_3 \leq 2\pi$. Since most of functions $f^{(q)}_{jk}$, $g^{(q)}_{jk}$, and $h^{(q)}_{jk}$ contain terms $e^{i\phi_1}$, $e^{-i\phi_1}$, $e^{2i\phi_1}$ or $e^{-2i\phi_1}$ as a coefficient,³⁰⁾ some elements of the correlation functions will become zero:

$$\begin{aligned} \langle f^{(q)}_{jk}{}^*(t+\tau) f^{(q)}_{lm}(t) \rangle &= 0 & \text{if } j \neq l \text{ and } k \neq m \\ & & \text{except for } j=l=5 \\ \langle g^{(q)}_{jk}{}^*(t+\tau) g^{(q)}_{lm}(t) \rangle &= 0 & \text{if } j \neq l \text{ and } k \neq m \\ & & \text{except for } j=l=5 \end{aligned}$$

Therefore, the products of these two elements become zero for $j \neq l$ and $k \neq m$. In this case Eq. (9) reduces to

$$\begin{aligned} & \langle F_q^*(t+\tau) F_q(t) \rangle \\ &= \sum_{j,k} \langle f^{(q)}_{jk}{}^*(t+\tau) f^{(q)}_{jk}(t) \rangle \langle g^{(q)}_{jk}{}^*(t+\tau) g^{(q)}_{jk}(t) \rangle \\ & \quad \times \langle h^{(q)}_{jk}{}^*(t+\tau) h^{(q)}_{jk}(t) \rangle \end{aligned} \quad (10)$$

This equation indicates that the overall correlation functions can be described as the sum of the products of the self-correlation functions for the respective motions without considering the cross terms appearing in Eq. (9). Therefore, we can simply make further calculation by using particular models to describe the motions for the respective moving units.

If we assume that the z_2 axis undergoes a spherical random reorientation in the laboratory frame, self-correlation functions of $h^{(q)}_{jk}(t)$ may be expressed by an exponential decay as

$$\langle h^{(q)}_{jk}{}^*(t+\tau) h^{(q)}_{jk}(t) \rangle = \langle |h^{(q)}_{jk}(t)|^2 \rangle e^{-|\tau|/\tau_l} \quad (11)$$

where τ_l is the correlation time for the isotropic motion and $\langle |h^{(q)}_{jk}(t)|^2 \rangle$ is deter-

mined to be 2/15 for all q 's using the equations listed in Table I of Ref. 30. Then Eq. (10) reduces to

$$\begin{aligned} \langle F_q^*(t+\tau)F_q(t) \rangle \\ = (2/15)e^{-|\tau|/\tau_l} \sum_j [\langle f^{(q)}_{jk}^*(t+\tau)f^{(q)}_{jk}(t) \rangle \\ \times \sum_k \langle g^{(q)}_{jk}^*(t+\tau)g^{(q)}_{jk}(t) \rangle] \end{aligned} \quad (12)$$

where $\langle f^{(q)}_{jk}^*(t+\tau)f^{(q)}_{jk}(t) \rangle$ are the same for all k values as indicated in the previous publication.³⁰⁾

We assume a three-fold rotation, which corresponds to the rotation of the α -CH₃ group about the C-C bond, as a model for the motion in frame S_1 . Following Woessner,³²⁾ we consider random jumps between three equilibrium positions ϕ_0 , $\phi_0 \pm 120^\circ$ to either of the two adjacent positions at an average rate of $(3\tau_R)^{-1}$. Straightforward calculations yield

$$\begin{aligned} \langle f^{(0)}_{jk}^*(t+\tau)f^{(0)}_{jk}(t) \rangle &= (3/4)C_R e^{-|\tau|/\tau_R} & \text{for } j=1, 2 \\ &= 3B_R e^{-|\tau|/\tau_R} & \text{for } j=3, 4 \\ &= A_R & \text{for } j=5 \\ \langle f^{(1)}_{jk}^*(t+\tau)f^{(1)}_{jk}(t) \rangle &= (1/12)C_R e^{-|\tau|/\tau_R} & \text{for } j=1, 2 \\ &= (1/12)B_R e^{-|\tau|/\tau_R} & \text{for } j=3, 4 \\ &= A_R & \text{for } j=5 \\ \langle f^{(2)}_{jk}^*(t+\tau)f^{(2)}_{jk}(t) \rangle &= (1/12)C_R e^{-|\tau|/\tau_R} & \text{for } j=1, 2 \\ &= (1/12)B_R e^{-|\tau|/\tau_R} & \text{for } j=3, 4 \\ &= A_R & \text{for } j=5 \end{aligned} \quad (13)$$

where

$$\begin{aligned} A_R &= (1/4)(3 \cos^2 \theta_R - 1)^2 \\ B_R &= 3 \sin^2 \theta_R \cos^2 \theta_R \\ C_R &= (3/4) \sin^2 \theta_R \end{aligned} \quad (14)$$

and θ_R is the supplementary angle of the bond angle of C-C-H associated with the α -CH₃ group, corresponding to the angle θ_1 .

As the motion of frame S_1 in frame S_2 , the rapid fluctuation of the z_1 axis is assumed about the z_2 axis, which corresponds to the random fluctuation of the rotation axis of the α -CH₃ group. Although this motion may differ in amplitude and frequency from the librational motion introduced in the previous work,³⁰⁾ the same equations can be used to describe the rapid fluctuation. Then the correlation functions for this motion are given by

$$\begin{aligned} \sum_k \langle g^{(0)}_{jk}^*(t+\tau)g^{(0)}_{jk}(t) \rangle &= 4[C_F + (1-C_F)e^{-|\tau|/\tau_F}] & \text{for } j=1, 2 \\ &= B_F + (1-B_F)e^{-|\tau|/\tau_F} & \text{for } j=3, 4 \\ &= 6[A_F + (1-A_F)e^{-|\tau|/\tau_F}] & \text{for } j=5 \\ \sum_k \langle g^{(1)}_{jk}^*(t+\tau)g^{(1)}_{jk}(t) \rangle &= 6[C_F + (1-C_F)e^{-|\tau|/\tau_F}] & \text{for } j=1, 2 \\ &= 6[B_F + (1-B_F)e^{-|\tau|/\tau_F}] & \text{for } j=3, 4 \end{aligned} \quad (15)$$

α -Methyl Group Rotation of Solid PMMA's

$$\begin{aligned}
 &= A_F + (1 - A_F)e^{-|\tau|/\tau_F} \quad \text{for } j=5 \\
 \sum_k \langle g_{jk}^{(2)*}(t+\tau) g_{jk}^{(2)}(t) \rangle &= 24 [C_F + (1 - C_F)e^{-|\tau|/\tau_F}] \quad \text{for } j=1, 2 \\
 &= 6 [B_F + (1 - B_F)e^{-|\tau|/\tau_F}] \quad \text{for } j=3, 4 \\
 &= 4 [A_F + (1 - A_F)e^{-|\tau|/\tau_F}] \quad \text{for } j=5
 \end{aligned}$$

where

$$\begin{aligned}
 A_F &= \cos^2 \theta_F (1 + \cos \theta_F)^2 / 4 \\
 B_F &= \sin^2 \theta_F (1 + \cos \theta_F)^2 / 6 \\
 C_F &= (\cos \theta_F + 2)^2 (\cos \theta_F - 1)^2 / 24
 \end{aligned} \tag{16}$$

and θ_F is the half of the vertical angle for a cone within which the rotation axis fluctuates at a rapid rate. Then the overall correlation functions are given by substituting Eqs. (13) and (15) in Eq. (12) as

$$\begin{aligned}
 \langle F_q^*(t+\tau) F_q(t) \rangle &= K_q [A_R A_F e^{-|\tau|/\tau_I} + A_R (1 - A_F) e^{-|\tau|/\tau_{FI}} \\
 &\quad + (B_R B_F + C_R C_F) e^{-|\tau|/\tau_{RI}} + \{ B_R (1 - B_F) + C_R (1 - C_F) \} e^{-|\tau|/\tau_{RFI}}]
 \end{aligned} \tag{17}$$

with

$$\begin{aligned}
 K_0 &= 4/5 \\
 K_1 &= 2/15 \\
 K_2 &= 8/15
 \end{aligned} \tag{18}$$

and

$$\begin{aligned}
 \tau_{FI}^{-1} &= \tau_F^{-1} + \tau_I^{-1} \\
 \tau_{RI}^{-1} &= \tau_R^{-1} + \tau_I^{-1} \\
 \tau_{RFI}^{-1} &= \tau_R^{-1} + \tau_F^{-1} + \tau_I^{-1}
 \end{aligned} \tag{19}$$

According to Eq. (2), the Fourier transformation of the correlation functions yields the following form of the spectral densities

$$\begin{aligned}
 J_q(\omega) &= K_q [A_R A_F J_I(\omega) + (A_R (1 - A_F) J_{FI}(\omega) + (B_R B_F + C_R C_F) J_{RI}(\omega) + \\
 &\quad \{ B_R (1 - B_F) + C_R (1 - C_F) \} J_{RFI}(\omega)]
 \end{aligned} \tag{20}$$

with

$$J_i(\omega) = 2\tau_i / (1 + \omega^2 \tau_i^2), \quad i = I, RI, FI, RFI$$

Although Eq. (20) is considerably complicated, it can be simplified when the correlation times for the respective motions significantly differ in order of magnitude from each other. For the motions of the α -CH₃ groups we can assume $\tau_I \gg \tau_R \gg \tau_F$ in the glassy state. Under such a condition Eq. (20) reduces to

$$J_q(\omega) = K_q [A_1 \{ 2\tau_F / (1 + \omega^2 \tau_F^2) \} + A_2 \{ 2\tau_R / (1 + \omega^2 \tau_R^2) \} + A_3 \{ 2\tau_I / (1 + \omega^2 \tau_I^2) \}] \tag{21}$$

with

$$\begin{aligned}
 A_1 &= B_R B_F + C_R C_F \\
 A_2 &= A_R (1 - A_F) + B_R (1 - B_F) + C_R (1 - C_F) \\
 A_3 &= A_R A_F
 \end{aligned}$$

As clearly seen from Eq. (21), contributions from the respective motions are described in terms of different Lorentzian functions. This results in Eq. (20) becoming model-free if coefficients A_1 , A_2 , and A_3 are assumed to be adjustable parameters for the analysis of spin parameters. In this paper, we refer to such a procedure as the model-free analysis. On the other hand, the application of the exact model is referred to as the model-dependent analysis hereafter.

EXPERIMENTAL

Samples. Three PMMA samples with different tacticities were used. Table I shows their triad tacticities, which were determined by the conventional ^1H NMR spectroscopy in solution, together with the abbreviation used to describe the samples. The molecular weights of the samples were estimated to be more than 500,000 by GPC. Each sample was hot-pressed at about 200°C under 138 MPa pressure into thin films and quenched in iced water.

Table I. Triad Tacticities of the Different Poly(methyl methacrylate)s

Sample	rr	mr	mm
s-PMMA	0.725	0.226	0.049
si-PMMA	0.495	0.157	0.348
i-PMMA	0	0	1.0

^{13}C NMR measurements. ^{13}C NMR measurements were performed on a JEOL JNM-FX200 spectrometer equipped with a CP/VT high-power probe or a CP/MAS probe for room temperature measurements under a static magnetic field of 4.7 T. A modified inversion-recovery pulse sequence shown in Figure 2 was used for the $T_{1\rho}$ measurements. The $\pi/2$ pulse widths of ^1H and ^{13}C radio-frequency fields were 3.6 and $3\ \mu\text{s}$, respectively, while the ^1H dipolar decoupling field $\gamma B_1/2\pi$ was reduced to 59 kHz. During the time interval τ introduced to leave ^{13}C magnetization to relax after the ^{13}C π pulse, which was generally set to 10–260 ms, a ^1H $\pi/2$ pulse train separated by 5 ms was used to saturate ^1H magnetization. The delay time PD after the acquisition of a free induction decay (FID) was set at least to $5 T_{1\rho}(1\sim 2\text{s})$ of the α -methyl carbon.

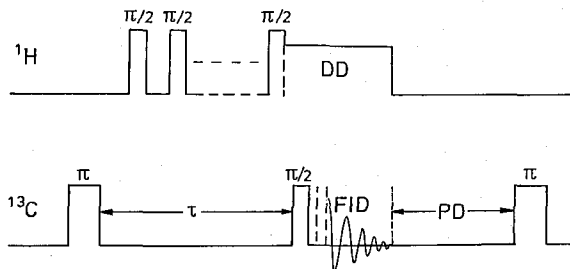


Fig. 2. Modified inversion-recovery pulse sequence used in this work.

Since other carbons have significantly longer T_{1C} values than the α -methyl carbon, the contributions from their resonances were successfully suppressed by setting such a short PD. The chemical shifts relative to tetramethylsilane (Me_4Si) were determined by using as an external reference the methyl line at 17.26 ppm of solid hexamethylbenzene for a CP/MAS ^{13}C NMR spectrum and the line at 128.5 ppm of liquid benzene for a CP/DD powder spectrum, respectively.

RESULTS AND DISCUSSION

Figure 3 shows 50 MHz CP/MAS ^{13}C NMR spectrum and CP/DD ^{13}C powder spectrum measured without MAS for i-PMMA at room temperature. The assignments of the resonance lines of the CP/MAS spectrum were made as shown in Figure 3, whereas in the CP/DD spectrum only lines of carbonyl carbons and α -methyl carbons could be unambiguously assigned. As seen in Figure 3(b), the contributions from other carbons severely overlap with the resonance line of the α -methyl carbon. However, by setting the delay time $\text{PD}=1\text{--}2\text{ s}$ in the modified inversion recovery pulse sequence, we could suppress the overlap of other lines for T_{1C} measurements of the α -methyl carbons (cf. Figure 1 in our previous paper²⁹). The exponential decay curves were obtained for the initial stage of the conventional plots of the peak heights of the α -methyl carbons and the T_{1C} values were determined from the initial slopes with an accuracy of 10–20% for the whole temperature range studied.

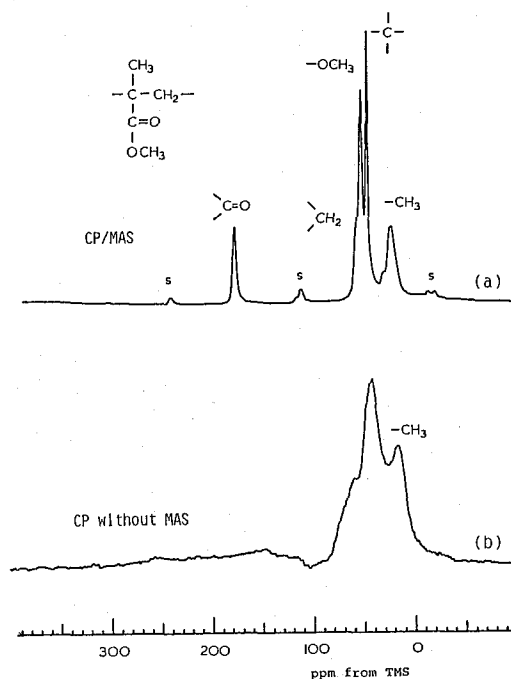


Fig. 3. 50 MHz CP/MAS ^{13}C MMR spectrum (a) and CP/DD powder spectrum (b) of i-PMMA at room temperature. S indicates a spinning side band.

In Figure 4 nT_{1C} values for the three PMMA samples are plotted against the reciprocal temperature ($1/T$), with the number n of protons chemically bonded to a carbon in question. In each case a marked but broad minimum can be observed; the fashion how the minimum appears significantly depends on the sample tacticity. For example, the T_{1C} value at the minimum increases with increasing isotactic content and the temperature giving the minimum is concomitantly shifted to a lower temperature. Such characteristic temperature dependences of the T_{1C} 's, especially the extraordinarily high values of T_{1C} 's at the minima, could not be interpreted in terms of the single-correlation-time model neither by introducing a box-type or $\log\chi^2$ distribution of the correlation times.

Model-Free Analysis

The solid curves in Figure 4 are the theoretical results obtained by the model-free analysis. Here we assume that the correlation time τ_R changes with temperature according to the Arrhenius equation, $\tau_R = \tau_{R0} \exp(\Delta E_R/RT)$, while τ_F is independent of temperature. Moreover, the contribution of the isotropic motion (Eq. (21)) is neglected because this motion is likely to be highly hindered in the glassy state. As clearly seen in Figure 4, the calculated curves fit well the experimental data points for these three samples. The temperature dependences of τ_F and τ_R , which were obtained by this analysis, are shown in the upper half of Figure 4. The activation energy ΔE_R

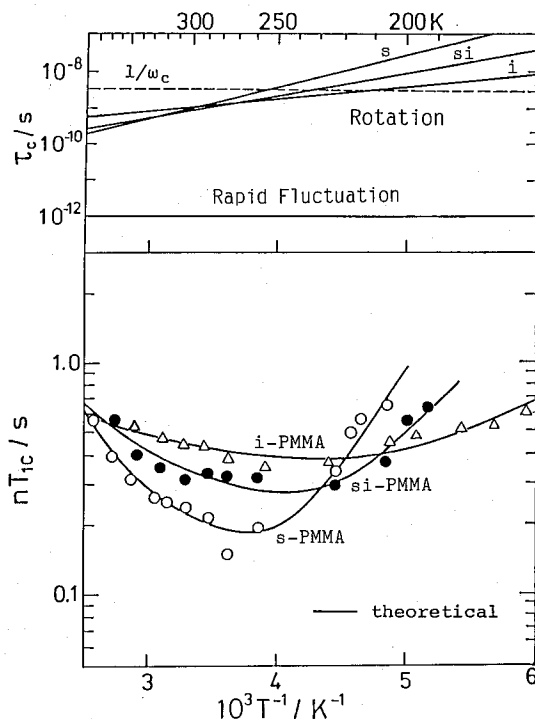


Fig. 4. nT_{1C} vs. $1/T$ for different PMMA samples and results of the model-free analysis.

Table II. Optimal Parameters Obtained by the Model-Free Analysis.

Sample	A_1	A_2	τ_{R0}^a/ps	$\Delta E^a/\text{kJmol}^{-1}$
i-PMMA	2.01	0.18	112.3	5.9
si-PMMA	0.23	0.27	6.93	12.0
s-PMMA	1.38	0.40	1.20	16.8

$$^a \tau_R = \tau_{R0} \exp(\Delta E/RT).$$

for the three-fold rotation of the α -methyl group and coefficients A_1 and A_2 in Eq. (21) are tabulated in Table II. According to this analysis, the activation energy of the α -methyl rotation is one of the most important factors determining the difference in temperature dependences of the T_{1C} 's, because the rapid fluctuation has the same correlation time of 10^{-12} s for these samples. The other factors closely associated with the T_{1C} results are A_1 and A_2 shown in Table II, although in the model-free analysis these coefficients are adjustable parameters only used in the least-square method by a computer. The apparent cause for the differences in A_1 and A_2 may be the difference in relative contributions of the methyl rotation and the rapid fluctuation to the relaxation but these parameters do not depend explicitly on the tacticity of the samples.

The activation energies for the α -methyl rotation have already been determined for PMMA's with different tacticities by ^1H NMR spectroscopy³³⁾ and quasi-elastic neutron scattering method:^{26,27)} 23–35 kJ/mol for syndiotactic PMMA and 16–23 kJ/mol for isotactic PMMA, respectively. These values are considerably higher than the values obtained from our ^{13}C NMR analysis, but there is the tendency that the activation energy increases with increasing syndiotacticity, which is common for the results obtained by different experimental methods.

Model-Dependent Analysis

Figure 5 shows the results of the model-dependent analysis where θ_R and θ_F were used as adjustable parameters in the least-square method instead of A_1 and A_2 in Eq. (21). The parameters obtained by this analysis are tabulated in Table III. As is clearly seen in Figure 5, the theoretical curves are in good accord with the observed values for i-PMMA and si-PMMA. Nevertheless, θ_R is much smaller than the complementary angle for the bond angle of C-C-H for these samples. Moreover, θ_F seems to be too large as an angle for the rapid fluctuation of the rotation axis, which corresponds to the local motion of the C-C backbone, in the glassy state. On the other hand, no better fit than the case shown in Figure 6 could be obtained for s-PMMA, although all possible values were examined for each parameter. These problems may suggest that only two superposed motions, the α -methyl rotation and the rapid fluctuation, are not enough to describe the temperature dependences of the T_{1C} values of the α -methyl carbons. The assumption of the independency of these two motions may be also unreasonable in the glassy state, although it seems to be very difficult not to make this assumption for the analysis. Further discussion will be made after more detailed data are obtained for the high-resolution line of α -methyl carbons by use of a magic-angle spinning technique at different temperatures.

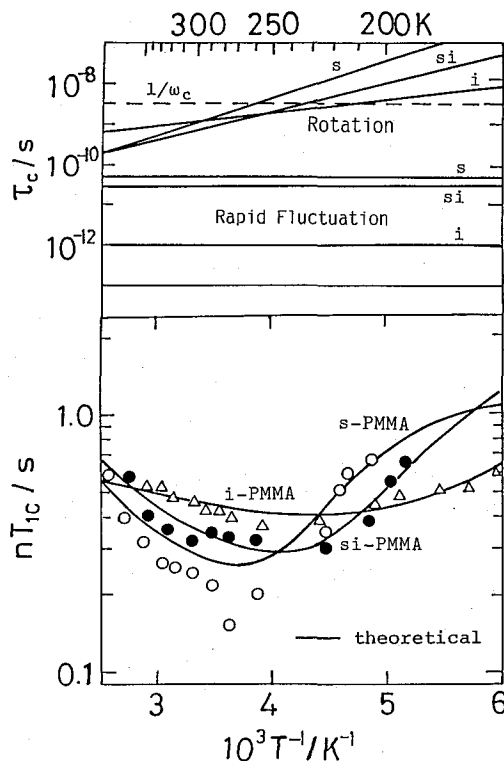


Fig. 5. nT_{1c} vs. $1/T$ for different PMMA samples and results of the model-dependent analysis.

Table III. Parameters Obtained by the Model-Dependent Analysis.

Sample	θ_F/degree	τ_F/ps	θ_R/degree	τ_{R0}^a/ps	$\Delta E^a/\text{kJmol}^{-1}$
i-PMMA	44.4	1.0	47.2	114.7	5.9
si-PMMA	63.4	30.0	47.3	4.00	13.2
s-PMMA	62.5	50.0	47.0	1.26	17.0

^a $\tau_R = \tau_{R0} \exp(\Delta E/RT)$.

REFERENCES

- (1) J. Schaefer and E. O. Stejskal, *Macromolecules*, **18**, 1031 (1976).
- (2) R. Kitamaru, F. Horii, and K. Murayama, *Macromolecules*, **19**, 636 (1986).
- (3) M. Nakagawa, F. Horii, and R. Kitamaru, *Polym. Prepr., Japan*, **35**, 3472 (1986).
- (4) F. Horii, Q. R. Zhu, M. Tsuji, and R. Kitamaru, *J. Soc. Rheology, Japan*, in press.
- (5) S. Saito, Y. Moteki, M. Nakagawa, F. Horii, and R. Kitamaru, *ACS Polym. Prepr.*, **29**, No. 1, 6 (1988).
- (6) F. Horii, T. Ito, and R. Kitamaru, *ACS Polym. Prepr.*, **29**, No. 1, 27 (1988).
- (7) F. Horii, S. H. Hu, T. Ito, H. Odani, R. Kitamaru, S. Matsuzawa, and K. Yamaura, *Polym. Prepr., Japan*, **37**, 2606 (1988).

α -Methyl Group Rotation of Solid PMMA's

- (8) A. Hirai, F. Horii, and R. Kitamaru, *Polym. Prepr., Japan*, **37**, 1156 (1988).
- (9) F. Horii, A. Hirai, and R. Kitamaru, *Macromolecules*, **20**, 2117 (1987).
- (10) F. Horii, H. Yamamoto, R. Kitamaru, M. Tanahashi, and T. Higuchi, *Macromolecules*, **20**, 2946 (1987).
- (11) F. Horii, Chapter 10 in *Application of Nuclear Magnetic Resonance in Agriculture*, P. E. Pfeffer, W. V. Gerasimowicz, Eds., CRC Press, Boca Raton, FL, in press; related references therein.
- (12) F. Horii, H. Yamamoto, A. Hirai, and R. Kitamaru, *Carbohydr. Res.*, **160**, 29 (1987).
- (13) D. L. VanderHart and R. H. Atalla, *Macromolecules*, **17**, 1465 (1984).
- (14) K. Murayama, F. Horii, and R. Kitamaru, *Polym. Prepr., Japan*, **31**, 2509 (1982).
- (15) F. Horii, K. Murayama, and R. Kitamaru, *ACS Polym. Prepr.*, **24**, 384 (1983).
- (16) F. Horii, A. Hirai, K. Murayama, R. Kitamaru, and T. Suzuki, *Macromolecules*, **16**, 273 (1983).
- (17) M. A. Desando, M. A. Kashem, M. A. Siddiqui, and S. Walker, *J. Chem. Soc., Faraday Trans. II*, **80**, 747 (1984) and references therein.
- (18) J. Williams and A. Eisenberg, *Macromolecules*, **11**, 700 (1978).
- (19) J. G. Powles, J. H. Strange, and D. J. H. Sandiford, *Polymer*, **4**, 700 (1963).
- (20) J. Humphreys, R. A. Duckett, and I. M. Ward, *Polymer*, **25**, 1227 (1984).
- (21) F. Heatley and A. Begum, *Polymer*, **17**, 399 (1976).
- (22) J. R. Lyerla, Jr., T. Horikawa, and D. E. Johnson, *J. Am. Chem. Soc.*, **99**, 2463 (1977).
- (23) J. Schaefer, E. O. Stejskal, and R. Buchdal, *Macromolecules*, **8**, 291 (1975).
- (24) H. T. Edzes, *Polymer*, **24**, 1425 (1983).
- (25) H. T. Edzes and W. S. Veeman, *Polym. Bull.* **5**, 255 (1981).
- (26) J. S. Higgins, G. Allen, and P. N. Brier, *Polymer*, **13**, 157 (1972).
- (27) G. Allen, C. J. Wright, and J. S. Higgins, *Polymer*, **15**, 319 (1974).
- (28) B. Gabrys, J. S. Higgins, K. T. Ma, and J. E. Roots, *Macromolecules*, **17**, 561 (1987).
- (29) B. Gabrys, F. Horii, and R. Kitamaru, *Macromolecules*, **20**, 176 (1987).
- (30) K. Murayama, F. Horii, and R. Kitamaru, *Bull. Inst. Chem. Res., Kyoto Univ.*, **61**, 229 (1983).
- (31) O. W. Howarth, *J. Chem. Soc., Faraday Trans. II*, **75**, 863 (1979).
- (32) D. E. Woessner, *J. Chem. Phys.* **36**, 1 (1962).
- (33) T. M. Connor and A. Hartland, *Phys. Lett.*, **23**, 662 (1966).